Nanofabrication, characterization and modeling of colloidal Au Nanoparticles

Alessandro Lovo Pierpaolo Ranieri

June 2020

1 Introduction

The aim of this experiment is the synthesis and characterization of colloidal spherical Au nanoparticles. The main steps followed by us were the synthesis using the chemical approach of the Turkevich method in aqueous solution, the measurement of the optical absorbance in the visible and near infra-red range of frequency and then a simulation with Mie theory in dipolar approximation to get information on the size and concentration of the nanoparticles and on the refractive index of the surrounding medium. Consequently we used the Grazing incidence X-Ray Diffraction (XRD) to obtain an independent measurements on the size of the particles and in the last part we did a morphological composition analysis with Scanning Electron Microscopy (SEM) with which it was possible to directly see and measure the nanoparticles.

2 Nanofabrication and Absorbance

2.1 Synthesis

The synthesys of the nanoparticles is performed via the Turkevich that reads as follows: the precursor used is a solution of $HAuCl_4$ which is heated up to 100°C. By adding sodium citrate ($Na_3C_6H_5O_7$), the precursor releases the gold forming a supersaturated solution and thus initiating the nucleation of the nanoparticles. Furthermore the citrate anions bind to the surface of the nanoparticle stopping their growth when they reach a radius of few nanometers.
By using a spectrophotometer it is possible to measure the absorbance spectrum of the solution with nanoparticles, which, after subtracting the contribution of the pure solvent is the one reported in fig 1. As can be seen, the spectrum exhibits a resonant behavior, and data near the peak can be used to estimate various properties of the system.

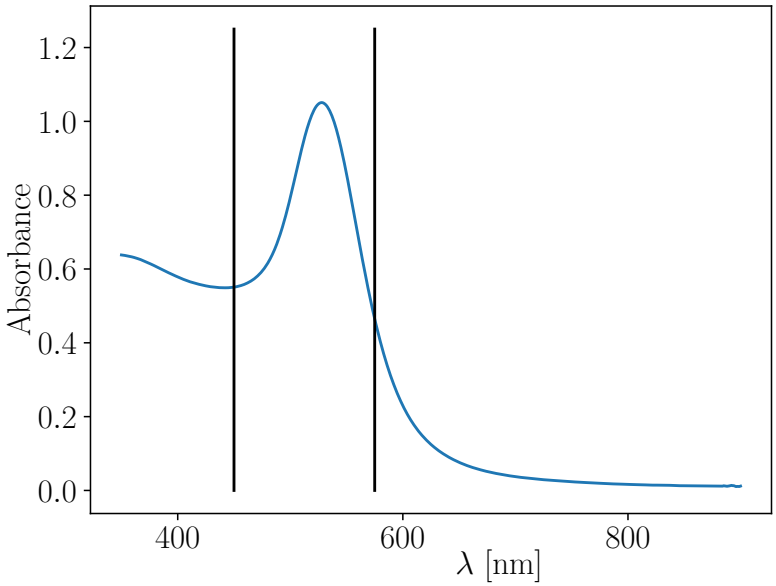

Figure 1: Absorbance spectrum of the nanoparticles and range used for the simulations: $\lambda \in [450, 575]$nm.

2.2 Optical characterization

From the Mie theory in dipolar approximation assuming non interacting spherical particles the formula for the absorbance is given by

$$A(\lambda; \epsilon_m, f) = \frac{18\pi}{\log 10} \frac{z}{\lambda} f \frac{\epsilon_m^{3/2} \epsilon_2(\lambda)}{(\epsilon_1(\lambda) + 2\epsilon_m)^2 + \epsilon_2(\lambda)^2}$$

where $z = 1$cm is the thickness of the sample, $f = \rho V$ is the filling fraction of nanoparticles, namely their numerical density ρ times their average volume V; ϵ_m is the dielectric constant of the medium surrounding the nanoparticles, while $\epsilon(\lambda) = \epsilon_1(\lambda) + i\epsilon_2(\lambda)$ is the dielectric constant of the nanoparticles, which in first approximation can be assumed to be the bulk one computed by Johnson and Christy (fig 3).
With this model there are only two free parameters: f and ϵ_m, so we tried values for them on a grid computing the reduced χ^2 of the simulation[1]. By defining

$$\chi_r^2(\epsilon_m, f) := \frac{\min_{\epsilon'_m, f'} \chi^2(\epsilon'_m, f')}{\chi^2(\epsilon_m, f)}$$

we obtained the plot in fig 2. The best values for the parameters are reported in tab 1.
Anyways from this simple fit not only there is a high uncertainty on the parameters, but most importantly there is no way to decouple the concentration of the nanoparticles from their size. For this reason is necessary to improve the model with the size correction.

[1]Since there are no errorbars on the datapoints $\{(\lambda_i, A_i)\}$ the χ^2 has been computed simply as $\chi^2 = \sum_i (A_i - A(\lambda_i))^2$

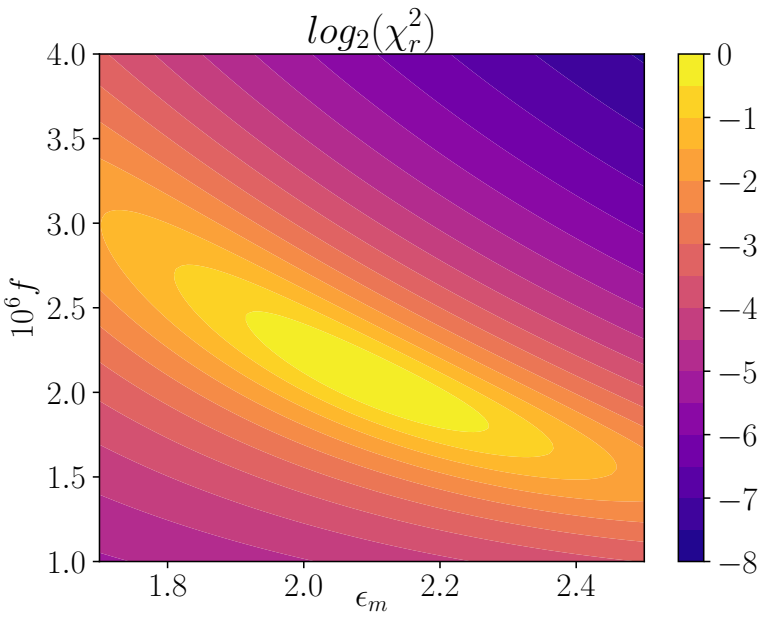

Figure 2: Map of the χ^2 with no size correction. With this type of visualization the curve at level $\log_2 \chi_r^2 = -1$ represents the region where the χ^2 is double than the minimum providing a natural confidence zone for the estimated parameters.

simulation method	$\min \chi^2/dof$	ϵ_m	f	R [nm]	ρ [µm^{-3}]
simple Mie theory	$8.74 \cdot 10^{-3}$	2.1 ± 0.3	$(2.1 \pm 0.5) \cdot 10^{-6}$		
size correction	$7.75 \cdot 10^{-4}$	2.04 ± 0.05	$(2.6 \pm 0.2) \cdot 10^{-6}$	6 ± 2	5 ± 5

Table 1: Best results from the simulations computed as $mean \pm \sqrt{variance}$

Size correction for ϵ From the Drude model for the electrons of the metal one can derive the following:

$$\epsilon_1(\omega, R) = \epsilon_1(\infty) + \omega_p^2 \left(\frac{1}{\omega^2 + \Gamma(\infty)^2} - \frac{1}{\omega^2 + \Gamma(R)^2} \right)$$
$$\epsilon_2(\omega, R) = \epsilon_2(\infty) - \frac{\omega_p^2}{\omega} \left(\frac{\Gamma(\infty)}{\omega^2 + \Gamma(\infty)^2} - \frac{\Gamma(R)}{\omega^2 + \Gamma(R)^2} \right)$$

where $\omega = c/\lambda$, R is the radius of the nanoparticle, ω_p is the bulk plasmon frequency and Γ is the typical damping time for electrons. With semiclassical computations one can find that

$$\Gamma(R) = \Gamma(\infty) + q\frac{v_F}{R}$$

where v_F is the Fermi velocity for electrons and $q = \pi/4$ in the assumption of spherical nanoparticles. The effect of the size correction can be seen in fig 3.
At this point the model has 3 free parameters (ϵ_m, f, R), that can be estimated with the same procedure as before. The best simulation is shown in fig 4(d).
As can be seen from tab 1 the results with this more sophisticated model are improved, but still the uncertainties are quite high (expecially the one of $\rho = f/\frac{4\pi}{3}R^3$). Also from the results

of the fit one can compute the index of refraction of the medium $n_m = \sqrt{\epsilon_m} \approx 1.43$ which is pretty high considering that the nanoparticles are in aqueous solution.

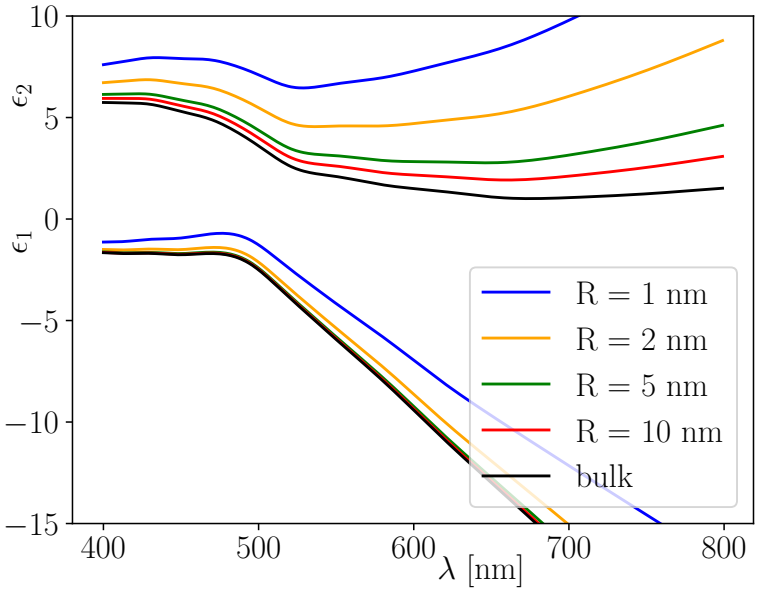

Figure 3: Real and imaginary part of the dielectric constant for gold at different nanoparticle sizes.

2.3 Possible sources of error and further improvements

Bulk parameters For the computations done here the bulk parameters for gold have been taken by the Ashcroft-Mermin textbook, but other sources give different values of them (tab 2), and hence different results. In particular since R enters the formula only as $\frac{v_F}{R}$ changing the Fermi velocity will heavily affect the determination of the size of the particles.
Moreover the bulk dielectric constant for gold $\epsilon(\omega, \infty)$ used here has been computed by Johnson and Christy via measurements on thin films of gold obtained by physical techniques, while the nanoparticles here studied have been synthesized chemically. So in principle this discrepancy can be a source of systematic error in the analysis.

Source	ω_p[Hz]	$\Gamma(\infty)$[Hz]	v_F[m/s]
Ashcroft-Mermin	$1.38 \cdot 10^{16}$	$1.08 \cdot 10^{14}$	$1.4 \cdot 10^6$
[1]	$1.3 \cdot 10^{16}$	$1.1 \cdot 10^{14}$	$0.94 \cdot 10^6$
[2]	$1.4 \cdot 10^{16}$	$1.1 \cdot 10^{14}$	$1.4 \cdot 10^6$

Table 2: Bulk parameters from different sources

Interacting nanoparticles All the computations done above assume that the nanoparticles do not interact with each other. This is a good approximation if $f < 0.1$ and since the data show $f \sim 10^{-6}$ the contribution of the interaction is surely negligible.

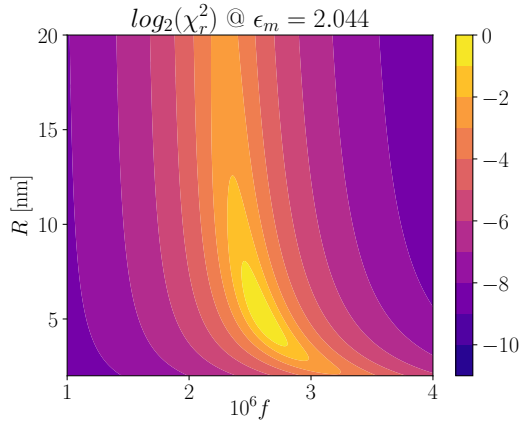

(a) χ^2 map at best value for ϵ_m

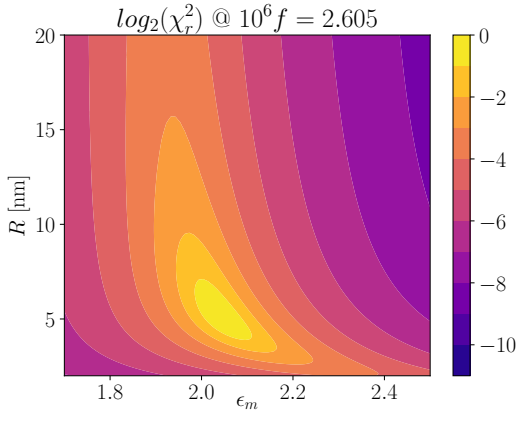

(b) χ^2 map at best value for f

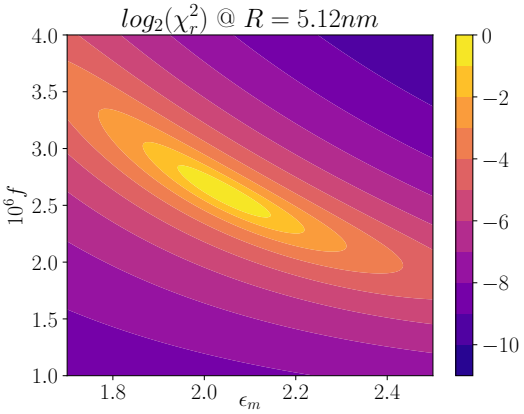

(c) χ^2 map at best value for R

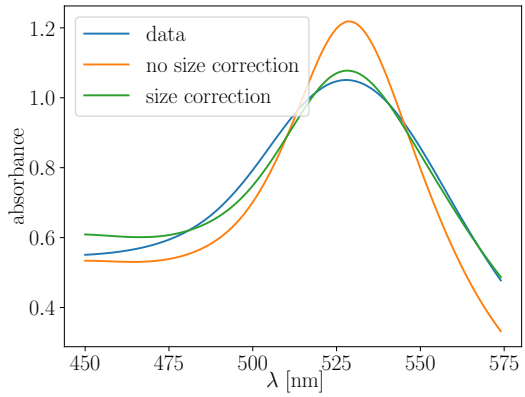

(d) Best simulation with and without size correction.

Figure 4: Results of the size corrected simulations.

Non-spherical particles It is possible to further refine the model by using Gans's theory instead of Mie's, namely considering the nanoparticles to be oblate ellipsoids with the new free parameter of the eccentricity e. Since for $e < 0.8$ the shape coefficient q in the size correction of ϵ varies less than 10% it is possible to simplify the computations using simply $q = \pi/4$. With this assumptions the model now reads:

$$A(\lambda; \epsilon_m, f, R, e) = \frac{2\pi}{3 \log 10} \frac{z}{\lambda} f \epsilon_m^{3/2} \epsilon_2(\lambda, R) \sum_{j=1}^{3} \frac{L_j^2}{\left(\epsilon_1(\lambda, R) + \epsilon_m \frac{1-L_j}{L_j}\right)^2 + \epsilon_2(\lambda, R)^2}$$

$$L_1 = \left(\frac{1}{e^2} - 1\right)\left(\frac{1}{2e} \log\left(\frac{1+e}{1-e}\right) - 1\right), \quad L_2 = L_3 = \frac{1 - L_1}{2}$$

Since now there are 4 free parameters, proceeding as before starts to be computationally expensive. For this reason to find the best combination of parameters we performed a Metropolis Monte Carlo walk on the parameter space considering the χ^2 as the potential energy to minimize, finding

$$\epsilon_m = 1.774,\ f = 2.81 \cdot 10^{-6},\ R = 11.7\,\text{nm},\ e = 0.66,\ \chi^2/dof = 5.09 \cdot 10^{-4}$$

Now we can happily notice that besides an improvement in the χ^2, the best value for ϵ_m yields a refractive index of $n_m = 1.33$, which is basically the one of water, and also the value for the size of the nanoparticles is more compatible with the one directly observed with SEM techniques (sec 4). On the other hand the value of the eccentricity is much higher than the one observed.
To better visualize the stability basin of this fit the χ^2 has been computed on a grid of values for R and e, proving to be again quite wide (figs 5(a),5(b)).

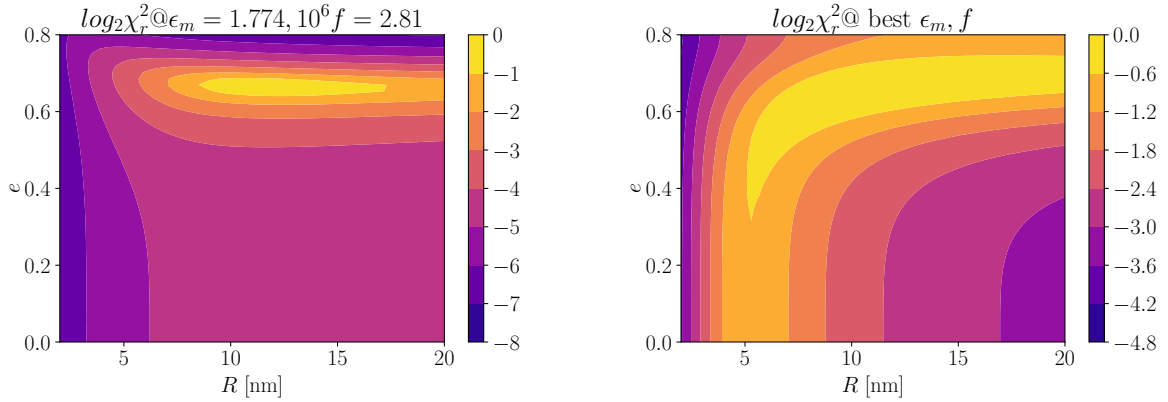

(a) χ^2 keeping ϵ_m, f fixed

(b) χ^2 minimized over ϵ_m, f

Figure 5: χ^2 map with shape correction

Non constant ϵ_m So far we have considered no dependence of ϵ_m on λ, but actually the refractive index of the medium can depend on the wavelenght and in first approximation one can use the first order Cauchy law:

$$\epsilon_m(\lambda) = n_m(\lambda)^2 = \left(n_0 + \frac{B}{\lambda^2}\right)^2$$

So now the model has five free parameters: n_0, B, f, R, e.
If one imposes $B >= 0$ (namely the refractive index decreases moving towards the infrared), the best combination of parameters has $B = 0$ and so the model reduces to the previous one. On the other hand letting B free the system finds a new equilibrium at

$$n_0 = 1.43,\ B = -6.72 \cdot 10^4 \text{nm}^2,\ f = 3.87 \cdot 10^{-6},\ R = 11.3\text{nm},\ e = 0.74,\ \chi^2/dof = 3.2 \cdot 10^{-5}$$

which allows the model to agree with the data even in the region at lower frequencies (thus lowering the χ^2 considerably), but comes with some issues: even ignoring the oddity of $B < 0$, the best value for the eccentricity is even higher than the one previously found and the refractive index of the medium around the peak in the absorption is $n_m(\lambda = 525\text{nm}) = 1.41$ which is again too high for an aqueous solution. For these reasons it is better to consider ϵ_m as constant.

Multipolar expansion All these computations have been performed using the dipolar approximation, so a further refinement of the model could be to include higher multipolarities. However, from the results obtained so far and by looking at the direct analysis of the SEM, $\lambda/R \approx 40$, which means that the contribution of higher multipoles should be negligible.

A posteriori size distribution By using the correlated distribution of size and eccentricity of the cluster $p(R, e)$ computed on the data from the SEM (fig 12(a)) we can fit only over ϵ_m, f with the following:

$$A(\lambda; \epsilon_m, f) = \frac{\int dRde\, A(\lambda; \epsilon_m, f, R, e)p(R, e)}{\int dRde\, p(R, e)} \approx \frac{\sum_{ij} A(\lambda; \epsilon_m, f, R_i, e_j)p(R_i, e_j)}{\sum_{ij} p(R_i, e_j)}$$

Where the integrals have been discretized since the distribution of R, e used is directly the histogram of the data. By doing so we find

$$\epsilon_m = 2.05,\ f = 2.36 \cdot 10^{-6},\ \chi^2/dof = 2.1 \cdot 10^{-3}$$

which is a result slightly better than the one with no correction at all, giving almost the same values for ϵ_m, f. On the other hand all the other *corrected* models fit better the data (fig 6).

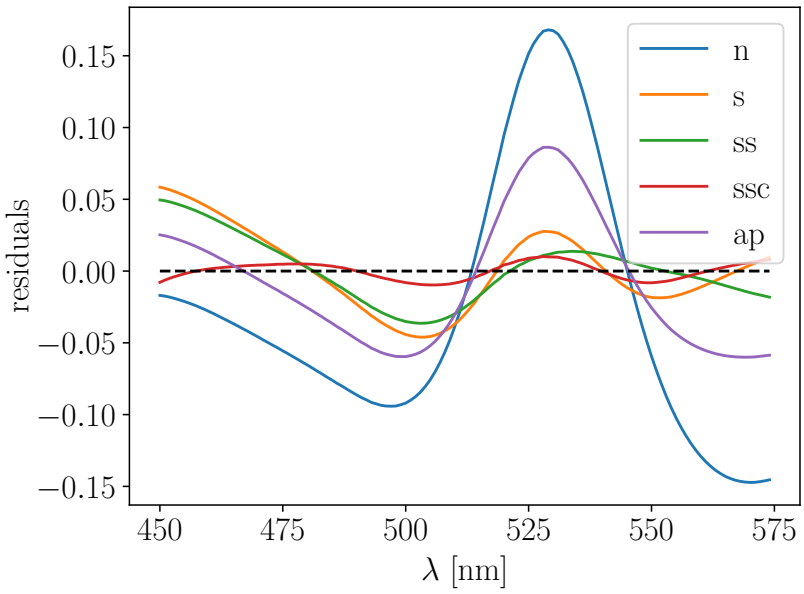

Figure 6: Residuals plot comparing the different models: no corrections (n), size correction (s), size & shape correction (ss), size, shape & Cauchy (ssc), a posteriori size & shape distribution (ap).

3 X-ray Diffraction

In this part we analyzed the X-Ray Diffraction pattern obtained by a diffractometer, depositing the nanoparticles, synthesized in the first part of the experiment, on a silicon substrate. In order to do the measurements we had to immobilize the particles on the silicon wafer surface with a suitable glue called APTES. With this method we had to choose the proper incident angle in order to enhance the signal from the nanoparticles and depress the one coming from the silicon substrate. The idea is to use grazing incidence, that is a small incidence angle in order to reduce the penetration depth in the substrate but not too much to avoid total reflection. Then we scan the 2θ angle from 30^o to 90^o, where 2θ is the angle formed between

the direction of the incident beam and the one of the diffracted one.
The acquired spectrum is reported in fig 7, that shows the intensity as a function of the angle 2θ. We fitted each peak with a pseudo-Voigt function in order to obtain information on the centroid and full width half maximum (FWHM) of each peak (tab 3). We can observe that all the peaks in the area from 50^o to 60^o should be disregarded because these are related to the silicon substrate.

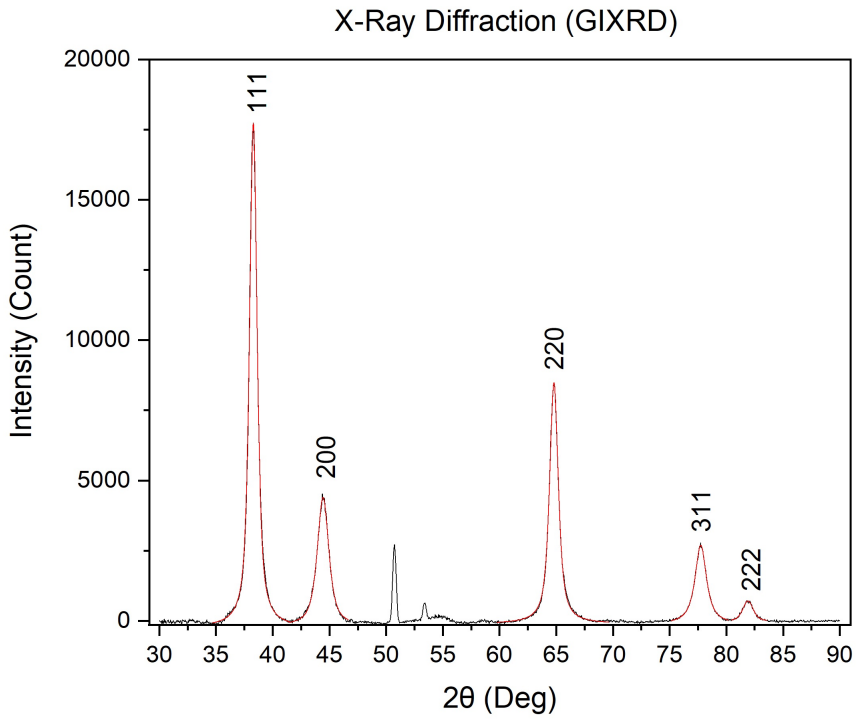

Figure 7: Spectrum of X-Ray diffraction obtained after removing the linear background. Each peak is fitted with a pseudo-Voigt function and labeled with its Miller indexes.

peak	2θ [degree]	FWHM [degree]	Net height	Area
1	38.28	0.803	17741.87	20357.91
2	44.43	1.218	4401.24	7991.70
3	64.79	0.917	8538.27	11276.67
4	77.74	1.209	2694.49	5145.29
5	81.90	1.092	686.15	1046.33

Table 3: Data obtained from the fit

Each peak is a maximum of diffraction of the wave and it is due to a plane with Miller indexes (h, k, l), which, in order to be consistent with the fcc structure of gold, must be all even or all odd. The distance between the planes is:

$$d_{(h,k,l)} = \frac{a}{\sqrt{h^2 + k^2 + l^2}} \tag{1}$$

where a is the lattice constant. Then we can calculate the inter-planar spacing d corresponding to each of those peak of equation 1 using the Bragg law:

$$d = \frac{\lambda}{2\sin\theta}$$

and we can compute the lattice parameter a comparing the results obtained with the bulk value ($a_{bulk} = 0.4065$ nm).
The size of the nanoparticles has been calculated using the Scherrer formula:

$$D_V = K\frac{\lambda}{\beta cos\theta}$$

where D_V is the volume-weighted crystallite size, $K = 0.89$ is the Scherrer constant, λ is the wavelength of the radiation ($Cu_{K\alpha 1} = 0.15406$ nm) and β is calculated in two ways: with linear or quadratic subtraction of the instrumental broadening β_{inst}

$$\beta = \beta_{obs} - \beta_{inst} \tag{2}$$

$$\beta = \sqrt{\beta_{obs}^2 - \beta_{inst}^2} \tag{3}$$

where β_{obs} is FWHM of the measured peaks. D_V could be considered as diameter of the nanoparticles.
All the results obtained are shown in tab 4.

peak	Miller indices	Lattice constant a [nm]	D_V (linear) [nm]	D_V (quadratic) [nm]
1	(1,1,1)	0.4069	15.61	11.00
2	(2,0,0)	0.4075	8.95	7.15
3	(2,2,0)	0.4067	14.38	10.62
4	(3,1,1)	0.4071	10.74	8.56
5	(2,2,2)	0.4071	12.66	9.83

Table 4: Results obtained from the XRD analysis.

We calculated the crystallite size for each peak but the most important information comes from the most intense peak (the one with miller indexes (1,1,1)). So we chose to take as best estimate for the radius the one corresponding to the first peak, from the linear calculation of the β (equation 2) we obtained R = 7.8 nm while from the quadratic one (equation 3) R = 5.5 nm.

Williamson-Hall analysis To improve our model we can consider also that the strain on the particles yields a peak broadening as well. With the Williamson-Hall analysis we are able to decouple the two sources of broadening. The Williamson-Hall relationship combining size and strain brodening is:

$$(\beta_{obs} - \beta_{inst})\cos\theta = K\frac{\lambda}{D_V} + 4\epsilon_{str}\sin\theta \tag{4}$$

In principle by performing a linear fit it is possible to estimate D_V and ϵ_{str}, but in our analysis we have too few peaks to obtain a meaningful fit (fig 8).

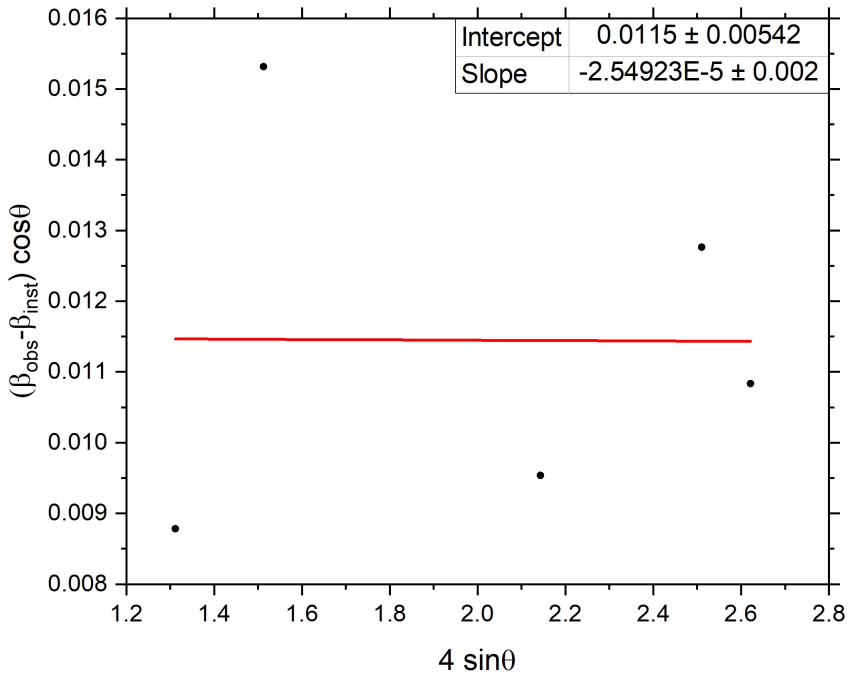

Figure 8

From the fit we obtain a crystallite size of D_V = 11.92 nm and a strain of ϵ_{str} = -2.5·10^{-5} rad. The fact that $\epsilon_{str} < 0$ confirms the ineffectiveness of this analysis for our sample.

4 Scanning Electron Microscopy

In this last part we performed a direct measurements of the size distribution of gold nanoparticles with scanning electron microscopy (SEM) on the same sample used for the XRD analysis. The image obtained with SEM is shown in fig 9.

We can see aggregates of particles due to the procedure used to attach them to the silicon substrate. This could lead to problems in the analysis because the program can not distinguish between two overlapped particles and an ellipsoidal one. Therefore we tried to neglect from the analysis with the software ImageJ all those shapes that seemed to be more than one particle. In order to do this we properly set the threshold on the gray scale to obtain a black and white contrast between the nanoparticles and the background and selected the part of the image that we were interested in analyzing, we then chose a minimum area of 30 nm^2 (corresponding to a radius of about 3 nm) and maximum 800 nm^2 (corresponding to a radius of about 16 nm) and a minimum circularity of 0.7. This allowed us to analyze a quite high number of particles (2358), sufficient to have an acceptable estimate of the average radius. In fig 10 is shown how particles have been selected for the analysis. The results obtained are shown in tab 5.

Number of cluster	R_{min} [nm]	R_{max} [nm]	$\langle R \rangle$ [nm]	$\sqrt[3]{\langle R^3 \rangle}$ [nm]	$\langle e \rangle$
2358	4.10	15.89	11.22	11.62	0.377

Table 5: Results obtained from the ImageJ program.

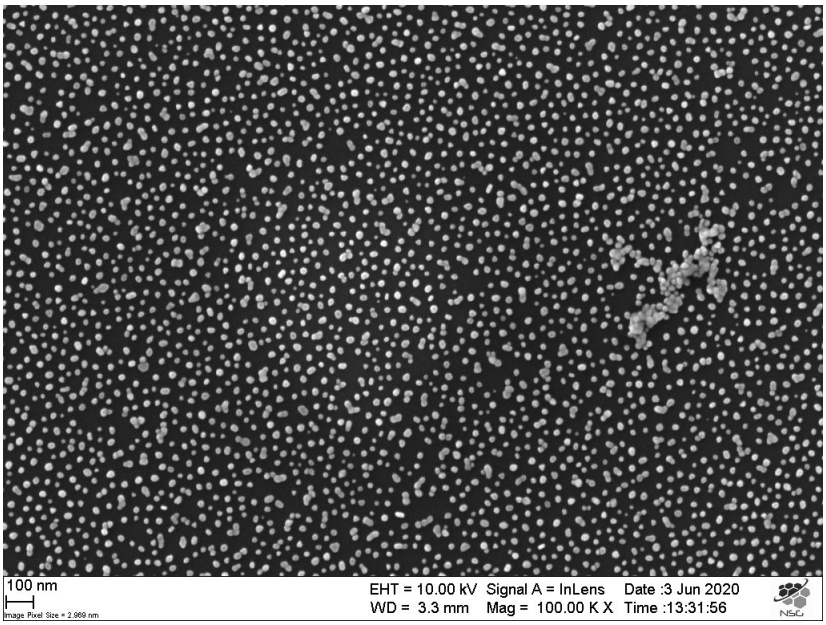

Figure 9: Gold nanoparticles on silicon substrate imaged with secondary electrons.

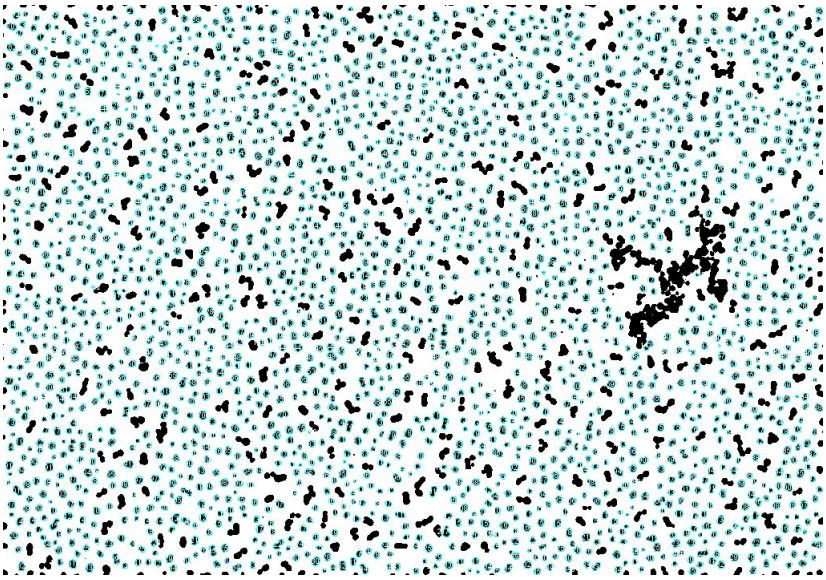

Figure 10: Example of how the particles have been selected. We can see that the bigger clusters have been excluded.

With the analysis done by the ImageJ program an histogram of the nanoparticles radius has been obtained, as shown in figure 11, fitted with a lognormal distribution. Also from the analysis of the particles it is possible to obtain an histogram of the eccentricity correlated with the distribution of the radius (fig 12(a), 12(b))

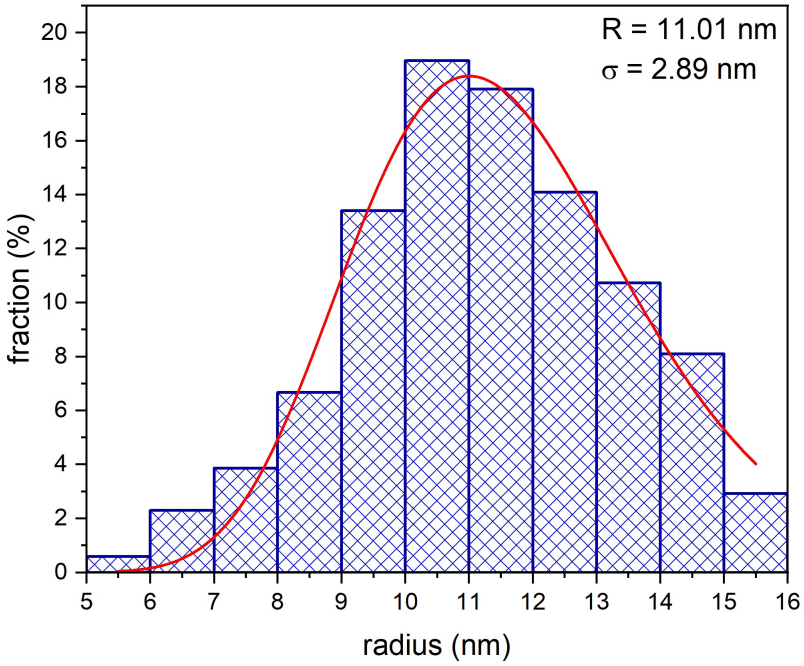

Figure 11: Histogram of the nanoclusters effective radius obtained from the ImageJ data.

From the lognormal fit we obtain a value of the radius of R = 11.01 nm where σ is the dispersion calculated as the standard deviation of the radius distribution.

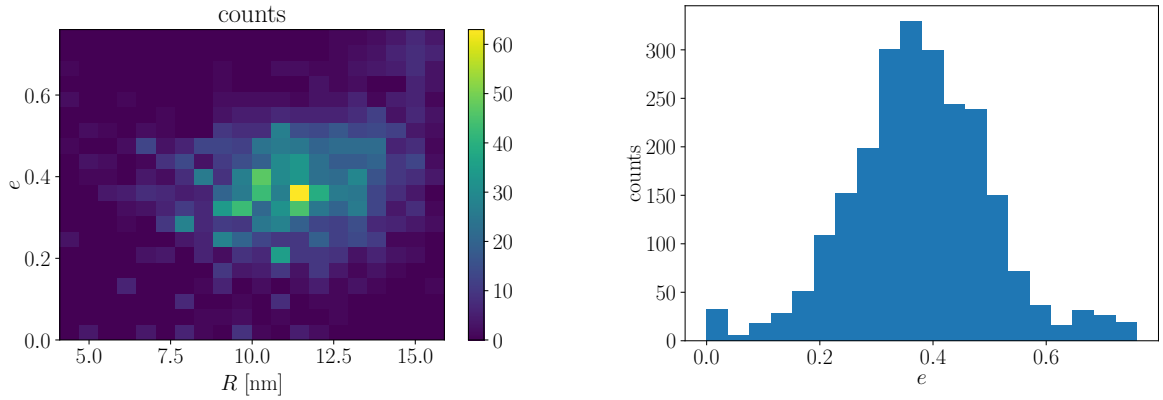

(a) Correlated distribution of R, e

(b) Distribution of the eccentricity

Figure 12: Histograms relating the eccentricity of the clusters. There is a positive correlation of 0.3 between R and e

5 Conclusions

With all three methods we analyzed the nanoparticles in different ways. The most significant analysis was the SEM with which we were able to directly measure the nanoparticle size, obtaining an estimate of the average radius of R = 11.22 nm.
With the XRD analysis conducted with the same sample analyzed with the SEM we obtained a smaller radius value, the most reliable measurement was probably the one in which the β was obtained by linear subtraction equal to R = 7.8 nm. With this analysis we also obtained information on the internal crystalline structure and we estimated the value of the gold lattice constant.
The anomalous result of different estimates of the nanoparticles' size using the same sample in the last two methods can be explained by the fact that the particles observed by the SEM are only a small portion of the ones analyzed with the XRD, and so, maybe, that portion is not representative of the whole. It is however interesting to notice that even though the Williamson-Hall analysis predicts odd results ($\epsilon_{str} < 0$), the value that it gives for R is perfectly compatible with the one observed on the SEM. Concerning the optical analysis of the nanoparticles the results with the simple size correction ($R \approx 5\,\text{nm}$) agree with the XRD prediction with quadratic subtraction of β_{inst} but disagree with the SEM results and also predict a very high index of refraction of the medium. On the other hand refining the model with also the shape correction yields a more reasonable value for the index of refraction and a better agreemnt with the SEM regarding the radius but overestimating the eccentricity. Anyways this is probably the best way to analyze the optical data since the discrepancy in the eccentricity can be explained considering that the SEM analysis is a 2D image and so what we measure is a *projected eccentricity* which in principle can be different from the true one.

In the end we can say that all the three experiments agree on the order of magnitude of the size of the nanoparticles and that, at the end of the day, the smaller discrepancies we observe are a symptom of reality being much more complicated than the models we use to describe it.

References

[1] `https://www.researchgate.net/figure/Optical-parameters-of-bulk-gold-used-and-determined-in-this-work_tbl1_231137746`

[2] `https://doi.org/10.1007/s11468-015-0128-7`